AIAA 2003–4947

Model of Current Collection to Small Breaches in Electrodynamic-Tether Insulation

Olivier Kern and Sven G. Bilén
The Pennsylvania State University, University Park, Pennsylvania 16802

39th AIAA/ASME/SAE/ASEE Joint Propulsion Conference and Exhibit
20–23 July 2003
Huntsville, Alabama

Model of Current Collection to Small Breaches in Electrodynamic-Tether Insulation

Olivier Kern*and Sven G. Bilén†

The Pennsylvania State University, University Park, Pennsylvania 16802

Future electrodynamic-tether missions are expected to be long duration (from several months to years); hence, these missions can expect possibly significant performance degradation due to breaches in tether insulating material caused by hazards such as micrometeoroids. In order to accurately predict this performance degradation, the collection of plasma current to these small breaches must be characterized. We have performed a series of plasma chamber experiments on simulated tether samples with holes in the outer insulation to determine I–V characteristics. The samples are fabricated from stainless-steel wire insulated with conventional shrink or Teflon tubing, and of annealed copper wire. Various sizes of breaches (holes) have been inserted in the insulation. The sizes of the holes, their number, and their spacing have been varied. The influence of the spacing on the current–voltage characteristic is compared to a developed model. The samples are connected to an electrometer so the I–V characteristic can be measured. Ionospheric-level plasma is generated with a low energy plasma source system running on argon. These results, while directly applicable to electrodynamic tethers, are also important for any insulated wiring on spacecraft that runs the risk of being impacted by micrometeoroids or small orbital debris.

Nomenclature

a	distance between adjacent pinholes, m
A_{eff}	effective sheath area, m^2
A_p	probe area, m^2
A_{sc}	"skull cap" area, m^2
b	insulation thickness, m
d_0	pinhole diameter, m
I	collected current, A
I_{oml}	oml current, A
j_{oml}	oml current density, A/m^2
k	subscript: i ions, e electrons
k_B	Boltzmann's constant, 1.38×10^{-23} J/K
L_0	characteristic object length, m
m_e	electron mass, 9.109×10^{-31} kg
m_i	ion mass, kg
n_∞	undisturbed plasma density, m^{-3}
q	charge magnitude, 1.602×10^{-19} C
q_k	k species charge, C
r_{eff}	effective radius, m
r_{eqcyl}	equivalent cylinder radius, m
r_h	hole radius, m
r_{infl}	radius of influence, m
r_p	probe radius, m
T_k	k species temperature, K
V_a	applied probe voltage, V
$\hat{V}_a$	normalized potential, dimensionless
V_p	plasma potential, V
v_{tk}	k species thermal velocity, m/s
ε_0	free space permittivity, 8.85×10^{-12} F/m
λ_D	Debye length, m
Ω	solid angle seen by pinhole, sr

*Graduate Research Assistant, Communications and Space Sciences Laboratory

†Assistant Professor, Communications and Space Sciences Laboratory, AIAA Member

Introduction

ELECTRODYNAMIC tether (EDT) systems have been proposed for long-duration missions lasting several months to many years.[1–3] These future EDT missions are of much longer duration than those of past and present missions, which were designed to last days or weeks. Although still a concern for short-duration missions, these longer missions will provide an especially harsh environment with respect to orbital debris.[4] Wider and/or multistrand tethers[5] may help mitigate against premature severing of the tether; nevertheless, the severity of the environment will result in tether performance degradation. Similar to the tether configuration employed on the upcoming ProSEDS (Propulsive Small Expendable Deployer System) mission,[6,7] these future EDT missions may employ partially bare, partially insulated configurations. It is estimated that the insulated and bare tether portions could receive hundreds to thousands of micrometeoroid hits over the course of a year-long mission. Although each of these hits may only be the size of a pinhole, these and larger "breaches" may affect the integrity of the tether and its operational capability.

In addition to the importance of understanding current collection behavior to pinholes on EDT systems, it is also relevant for defects in insulated wiring of large space power systems in low Earth orbit, such as that on the International Space Station. At best, such pinholes represent a loss of available power to the

spacecraft, but they can lead to breakdown and arcing at the triple point established between the plasma, metal, and dielectric.[8] Although primarily applied to small holes in flat insulated surfaces, the research performed to date has attempted to address both of these issues via theoretical,[9, 10] numerical,[11] and experimental[8, 9] methods.

In this work, we seek the following goals. First, we wish to characterize the influence of a single pinhole in the insulation of an insulated conductor immersed in plasma. We wish to determine if the current collected by this pinhole can be related to known collection models and to characterize the influence of the size of the hole, the size of the conductor, and the thickness of the insulation. We also wish to determine the role of the insulation in charge collection. Finally, we wish to determine the interaction between several pinholes and measure how pinhole spacing affects the collected current.

Background
Micrometeoroids and Orbital Debris

Single-line tethers can be quickly severed by micrometeoroids. The space environment above the earth is cluttered with millions of naturally occurring micrometeoroids as well as man-made orbital debris. Meteoroids are solid particles of extraterrestrial origin present in interplanetary space and in the Earth's vicinity. Most of them are particles ejected from collisions between asteroids or are particles ejected by cometary nuclei upon their closest approach to the Sun. Doppler observations—now available with speed resolutions of <10 m/sec for meteor speeds up to nearly 100 km/sec—give an average measured micrometeoroid velocity around 50 km/s.[12] Due to the typically long physical length of tethers, there is a high probability of being hit by these dust particles, which modifies the electrical interaction between tethers and the surrounding plasma, particularly if the impact breaches the insulation.

Although the exact impact process is not yet well known, it is thought that, due to the high impactor velocity, the large kinetic energy is converted to heat that turns the impactor into an exploding ball of plasma.[13] This assumption is grounded in the fact that the returned plates from the Long Duration Experiment Facility (LDEF) show nearly perfect melted hemispheres. If the impact dynamics were bullet like, one would expect an ellipsoidal impact shape due to the projectile plowing into the surface at an angle.

In this work, we consider breaches made by particles that do not sever the tether. (If a single-line tether were cut, we should be able to detect that through a change in tether dynamics.) We wish to determine how damaged an insulated conducting tether is. We also wish to examine current collection by a severed line in a multi-line tether.

Current Collection Theory

The current collected by a metallic probe in plasma can be described by two theories: Child–Langmuir (CL) and orbital-motion-limited theory (oml). CL theory applies when the characteristic object length (L_0) is large compared to the Debye length (λ_D), i.e., $L_0 \gg \lambda_D$; oml theory applies when $L_0 \ll \lambda_D$. Our study focuses on oml current collection since, in general, the oml regime is relevant for electron current collection to bare EDTs.[14–16]

Orbital-motion limited theory provides a model for the current collected by cylindrical and spherical probes. In oml theory, the number of particles collected by a probe is derived from considerations of energy and angular momentum only. Neglecting collisions and plasma directed velocity, as would exist on orbit, the current collected by a cylindrical conductor is given by

$$I_{\text{oml}} = q_k n_\infty A_p v_{tk} \frac{\sqrt{2}}{\pi} \sqrt{1 + \frac{qV_a}{k_B T_k}}, \qquad (1)$$

where the subscript k stands for i or e, depending on the attracted species, ions or electrons, respectively; q is the particle charge; n_∞ is the unperturbed particle density; A_p is the area of the probe; $v_{tk} = \sqrt{k_B T_k/m_k}$ is the thermal velocity of the collected species; k_B is Boltzmann's constant; V_a is the applied potential; and T_k is the attracted species temperature. For a sphere, the current collected is given by

$$I_{\text{oml}} = q_k n_\infty A_p v_{tk} \sqrt{\frac{2}{\pi}} \left(1 + \frac{qV_a}{k_B T_k} \right). \qquad (2)$$

Pinhole Collection Model

We wish to establish a model for the current collection due to a pinhole in the tether insulation. We assume that we have oml current collection, which we can do so since we know the geometry of our system and the plasma characteristics. We neglect collisions and assume no plasma flow or magnetic field. The two last assumptions are true in our experimental setup, but for a real orbital system they do not hold. We introduce here the concept of radius of influence, r_{infl}. We have seen in Eq. (2) that, for a sphere of radius r_p, the collected current is

$$I_{\text{oml}} = 4\pi r_p^2 j_{\text{oml}} = 4\pi r^2 q_k n_\infty v_{tk} \sqrt{\frac{2}{\pi}} \left[1 + \hat{V}_a \right],$$

where $\hat{V}_a = q(V_a - V_p)/k_B T_k$, with V_p being the plasma potential. If we define the radius of influence as

$$r_{\text{infl}} = r_p \sqrt{\sqrt{\frac{2}{\pi}} \left[1 + \hat{V}_a \right]}, \qquad (3)$$

then

$$I_{\text{oml}} = 4\pi r_{\text{infl}}^2 j_{tk}, \qquad (4)$$

where $j_{tk} = q_k n_\infty v_{tk}$ is the thermal current density. Thus, our pinhole appears as if it were a sphere of radius r_{infl} that is simply collecting the thermal current density. This concept allows us to use a straightforward model for two "close" pinholes. For a single probe (i.e., single pinhole), the collected current is the product of the thermal current and the area of a sphere with radius r_{infl}. For two probes, however, what is the collected current? If the probes are far away, i.e., they do not influence each other, the current collected will be twice that collected by a single probe. If the probes are infinitely close, i.e., touching, they will tend to collect the same current as a single probe of double area. We postulate that a good approximation to determine the current collected by two close spherical probes in between these two extremes is to use the concept of radius of influence. The collected current is the product of the thermal current times the remaining sphere of influence.

The current collection model is based on the geometry of the probe. Analytical solutions are available for simple geometries, i.e, planar, cylindrical, or spherical. Does a pinhole in the insulation of a conducting wire follow one of these collection regimes? We postulate that the current collected follows the spherical collection regime. As we shall see, this assumption was verified via experiment. Here, we make the assumption that pinholes collect current as a spherical probe with equivalent area.

We wish to find the equivalent spherical probe radius of a pinhole. We assume that the collection regime is spherical in nature, and that if the pinhole is small enough, it will only see the plasma with a solid angle of $\sim 2\pi$. So the area of the pinhole, πr_h^2, has to be equal to half the area of the equivalent sphere, i.e., $\pi r_h^2 = \frac{1}{2}\left(4\pi r_{\text{eff}}^2\right)$, which leads to the result that a pinhole of r_h has an effective radius of

$$r_{\text{eff}} = \frac{r_h}{\sqrt{2}}. \qquad (5)$$

Array of Pinholes

We consider an infinitely long tether where all the pinholes are aligned and equally spaced. Let a be the distance between two consecutive holes. Let us consider a section of wire of length a, since that is the smallest spatial period. A single hole will collect one half of the current collected by a sphere of radius r_{eff}, since it only sees the plasma with a solid angle of 2π. The sheaths of influence will overlap if the potential is increased past a threshold value. The limit is found by solving

$$a = 2r_{\text{infl}} = 2r_{\text{eff}}\sqrt{\sqrt{\frac{2}{\pi}}\left[1 + \hat{V}_a\right]} \qquad (6)$$

for $\hat{V}_a$, which yields a normalized applied voltage of

$$\hat{V}_a = \left[\left(\frac{a}{2r_{\text{eff}}}\right)^2\sqrt{\frac{\pi}{2}} - 1\right]\frac{k_B T_e}{q} \qquad (7)$$

at the threshold for overlapping spheres.
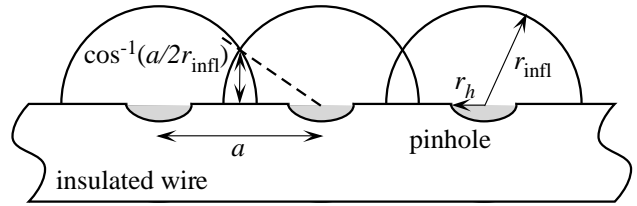
Fig. 1 Sketch of overlapping spheres of influence.

When the overlapping occurs (Fig. 1), we have to remove from the total sheath area two "skull caps", since they exist on both sides of the sheath. The area of the half sphere's skull caps that intersect is

$$
\begin{aligned}
A_{sc} &= \int_0^\pi r_{\text{infl}}d\phi \int_0^{\cos^{-1}(a/2r_{\text{infl}})} r_{\text{infl}}\sin\theta d\theta \\
&= \pi r_{\text{infl}}^2\left(1 - \frac{a}{2r_{\text{infl}}}\right).
\end{aligned} \qquad (8)
$$

On the length a, the area formed by the sheath of influence denoted A_{eff} is

$$A_{\text{eff}} = 2\pi r_{\text{infl}}^2 - 2\pi r_{\text{infl}}^2\left(1 - \frac{a}{2r_{\text{infl}}}\right) = \pi r_{\text{infl}}a, \qquad (9)$$

with

$$r_{\text{infl}} = r_{\text{eff}}\sqrt{\sqrt{\frac{2}{\pi}}\left[1 + \hat{V}_a\right]} = \frac{r_h}{\sqrt{2}}\sqrt{\sqrt{\frac{2}{\pi}}\left[1 + \hat{V}_a\right]}. \qquad (10)$$

The collected current is then given by

$$I = A_{\text{eff}}j_{tk} = \pi a r_{\text{infl}}j_{tk}. \qquad (11)$$

If the potential is less than the value given by Eq. (7), then the current collected is simply

$$I = j_{tk}2\pi r_{\text{infl}}^2. \qquad (12)$$

To illustrate this model, we consider equally spaced holes of radius r_h separated by $a = 50r_h/\sqrt{2} = r_{\text{eff}}$, with electron temperature of $T_e = 0.1$ eV. The voltage $\hat{V}_a$ at which the collection regime switches is given by Eq. (7) and is ~ 78 V. We obtain the I–V characteristic of Fig. 2 for saturation current levels, that is, not valid in the retardation regime.

This model makes physical sense at the limits. When the applied potential is small, the pinholes are independent. When the potential is large enough that the sheaths begin to overlap, the power of r_{infl} switches from two to one, i.e., the I–V curve characteristic
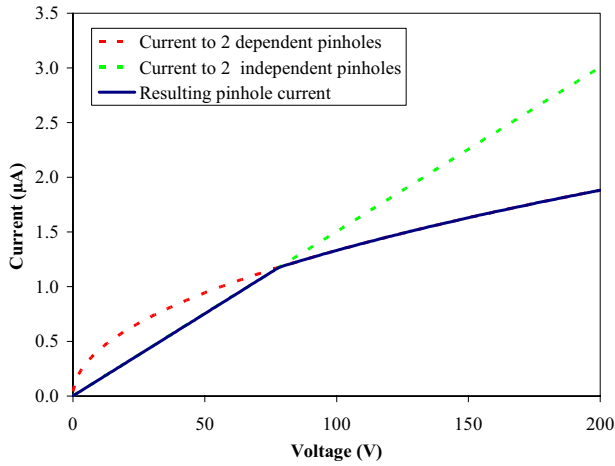
Fig. 2 **I–V characteristic of a section of insulated tether of length a with an array of pinholes. The radius of each pinhole is r_h; separation distance is set to $a = 50r_{\text{eff}}$. Shown plotted is current collected by two independent pinholes, current collected by dependant pair of pinholes, and total resulting current from one regime to the other.**

changes from linear to square-root. In other words, when the holes start to interact, the nature of the current collection switches from spherical to cylindrical. To see the equivalent cylinder, we may consider the ratio

$$\frac{I}{j_{\text{oml}}} = 2\pi r_{\text{eqcyl}} a = \frac{j_{tk} \pi r_{\text{infl}} a}{j_{tk} \frac{2\sqrt{2}}{\pi} \left[\sqrt{\hat{V}_a} + 1 \right]} = \frac{\pi}{2} \sqrt[4]{\frac{2}{\pi}} r_h a, \tag{13}$$

which yields

$$r_{\text{eqcyl}} = \frac{1}{4} \sqrt[4]{\frac{2}{\pi}} r_h \approx 0.2233 r_h. \tag{14}$$

The pinhole array behaves as a cylinder of radius r_{eqcyl} for large enough voltage. The radius of the equivalent cylinder is proportional to the radius of the pinhole, not of the cylinder. However, the pinholes have a cylindrical-like current collection with collection area defined by the pinhole dimensions.

Experimental Setup
Chamber Description and Setup

For our experimental investigations, we used the CSSL plasma chamber at Penn State (Fig. 3). It is a 1-m long, 0.6-m diameter stainless-steel cylinder in which a cryogenic pumping system lowers the pressure to $\sim 10^{-7}$ torr. The Earth's magnetic field is not compensated. To reproduce realistic space conditions, a plasma is created in the chamber using a hollow cathode. The plasma is generated by an Electric Propulsion Lab (EPL) low energy plasma source (LEPS) System 250. The LEPS 250 system is capable of providing a high flux of low energy ions and was

designed for volume plasma generation. It was run with argon gas and provided ions with $\sim$20 eV energy and electron energies $\sim$1 eV. The plasma environment is measured with a Langmuir probe system consisting of a metallic probe attached to a source electrometer. For our experiments, the plasma density was about $\sim 10^{13}$ m^{-3} and an electron temperature of ~ 11600 K. These numbers are about an order of magnitude higher than the ionospheric plasma at an altitude of 400 km, but their ratio, which determines the Debye length, is about the same, where Debye length is given by

$$\lambda_D = \sqrt{\frac{\varepsilon_0 k_B T_e}{q_e^2 n_e}}. \tag{15}$$
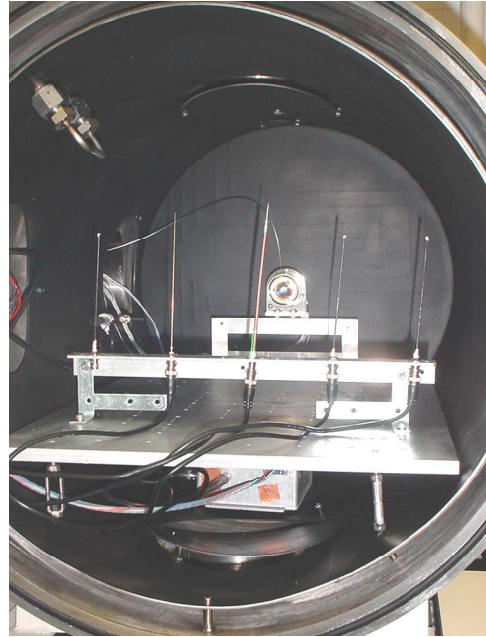
Fig. 3 **Internal view of the CSSL plasma chamber showing the LEPS 250 plasma source and test setup to determine the current collected to holes in insulated tether samples.**

Samples

The samples are all insulated conductors that are soldered into a BNC connector and then connected to a source electrometer via a switching network. A layer of epoxy on both ends of the conductor ensures no contact with the surrounding plasma other than at desired locations. Holes are then drilled in the insulation using a high speed milling system, which is precise and repeatable (within 0.006 mm or 0.25 mils). The conductor used is either a 35-mil-diameter (0.89-mm) stainless-steel wire or a 32-mil-diameter copper conductor. The insulation for the stainless-steel bar is either Teflon tubing or commercial-grade polyolefin. The copper conductor (magnet wire) has a thin layer of oleoresinous insulation. Fig. 4 shows a magnified view of a sample with machined pinholes.
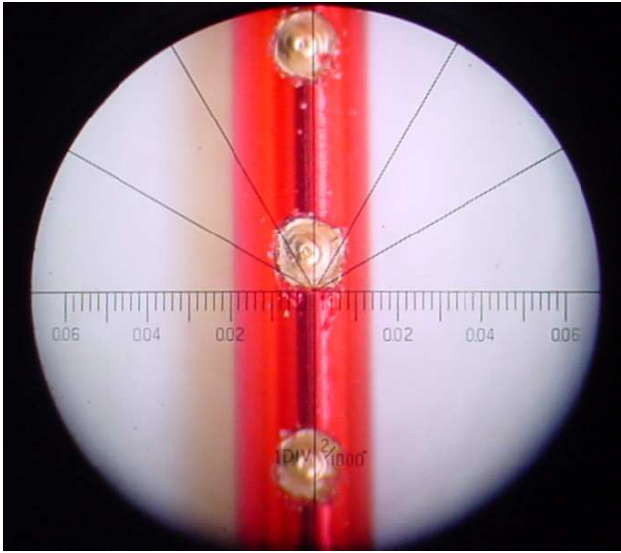
Fig. 4 Magnified view of 15-mil holes drilled through the insulation of an annealed wire sample. One division corresponds to 2 mils (5.08×10^{-5} m).

Experimental Results

Current Collection Mode for Pinholes

We wish to determine the current collection mode of a pinhole. Therefore, we compare the shape of the current collected by a single hole and by a cylindrical plasma probe. We have ruled out planar (thin sheath) collection *a priori*. Fig. 5 shows the normalized I–V curve from a single hole of diameter 20 mil drilled in the insulation of the 32-mil magnet wire and the normalized I–V curve from the cylindrical Langmuir probe. (The currents of the probe and pinhole sample were normalized at the plasma potential.) We see that the LP current follows a cylindrical response, as expected, whereas the pinhole follows a spherical response. Other researchers, such as *Galofaro*,[11] have made this assumption in their numerical simulations of current collected by a single pinhole on an insulated cable.

Fig. 6a shows current–voltage data for several different sized pinholes. In this particular experiment, 11-, 15-, and 20-mil holes were drilled into Teflon insulation with 6-mil thickness.

Solid-Angle Shadowing Effect

Although the collecting area has a spherical behavior, we must adapt the spherical current collection theory to our specific configuration. As a first approximation, we stated previously that instead of a 4π solid angle seen by a sphere, the space seen is more on the order of a 2π solid angle; however, the exact value must be experimentally determined. We discuss later a scale factor relating the dimension of the hole and the dimension of an equivalent collecting sphere. Here we assume only that they are related by some scale factor. Making this assumption, we expect that the
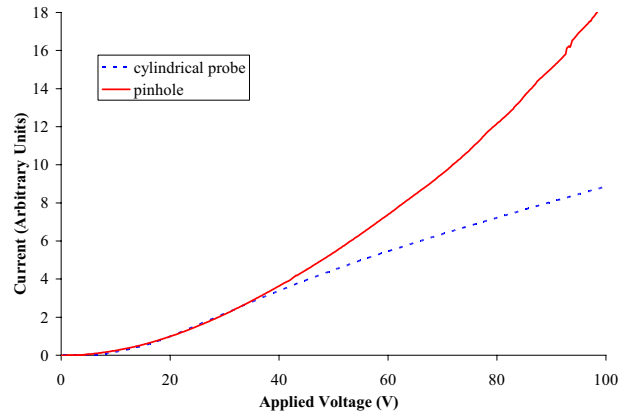

Fig. 5 Normalized I–V curves obtained for a cylindrical Langmuir probe and for a single 11-mil diameter hole drilled in Teflon tubing around a 35-mil diameter stainless-steel wire.

current collected by holes drilled on identical samples would be proportional to the square of the holes' radii.

In addition to scaling to account for hole size, we also must introduce the concept of solid-angle shadowing. Previously, we had assumed ideal holes in infinitely thin insulation. In practice, however, the insulation has a non-negligible thickness. Fig. 7 illustrates the plasma shadowing due to the insulation. The solid angle seen by the exposed conductor is

$$\Omega = \int_0^{2\pi} \int_0^{\tan^{-1}(2r_h/b)} \sin(\theta) d\theta d\phi$$
$$= 2\pi \left[1 - \cos\left(\tan^{-1}\left(\frac{2r_h}{b} \right) \right) \right]. \quad (16)$$

Hence, if this construct is correct, then in order to superimpose the curves from different holes, we should not only divide by the square of the holes' radii, but also by the respective solid angle given by Eq. (16). Fig. 6b shows the curves obtained when we normalized with respect to the radius and shadowing effects. Although the agreement is good for the two larger holes, we can see that it is not for the smallest hole, indicating that other effects may also be important at very small hole sizes.

Role of Charged Insulation

To understand how an insulated object containing a pinhole collects current, we must understand how it relates to a similar object of equivalent geometry and dimensions but without insulation on its surface. The presence of the insulation around the pinhole plays an important role. To illustrate is, let us assume that the conductor is at a potential higher than the surrounding plasma. Due to this potential difference, charges accumulate on both sides of the insulation—opposite charges on either side of the dielectric similar to a capacitor. The charge distribution is not homogenous
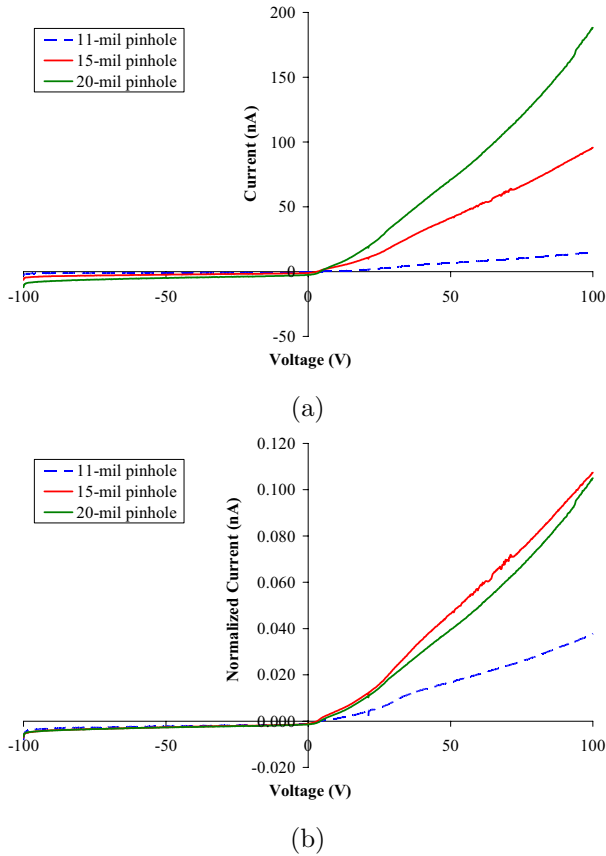
Fig. 6 (a) I–V curves obtained for single holes of diameters of 11 mil, 15 mil, and 20 mil drilled in Teflon tubing around a 35-mil diameter stainless-steel wire. (b) Normalized I–V curves obtained dividing data in (a) by 11^2, 15^2, and 20^2, respectively, and taking into account shadowing.
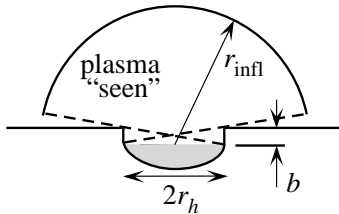

Fig. 7 Sketch of a section of wire with a hole of diameter $d_0 = 2r_h$ in the insulation. Due to the insulation's thickness b, the collecting area sees the plasma with a solid angle $< 2\pi$.

and is not easy to calculate analytically. Its precise determination requires extensive computer calculations of particle orbits in the anticipated geometries and electric fields using codes such as NASCAP/LEO[11] or particle-in-cell codes.

Due to the presence of the insulation surrounding the bare area, the electric field lines are perturbed, which affects the apparent collecting area. The charge accumulating on the insulation shields the plasma from the potential applied. This shielding has a spatial dimension of the order of a Debye length. As a result, the collected area tends to be partly shadowed by the charge gathering on the insulation. We can surmise that the dependency should be related to the voltage, hole size, and Debye length.

Fig. 8 illustrates the capacitor concept described previously. We used a stainless-steel wire insulated with Teflon shrink-tube insulation and drilled a single small hole. We applied a 100-V potential to the bar and recorded the resulting collected current. There is a relaxation time on the order of 3 seconds, which is an "eternity" for the plasma. This relaxation time shows the existence of a resistor–capacitor behavior, the resistance being the plasma itself, the capacitor being due to the accumulation of charge on both sides of the insulation as described previously. Similar observations have been made by *Vayner et al.*[8] who observed relaxation times of about 10 seconds.
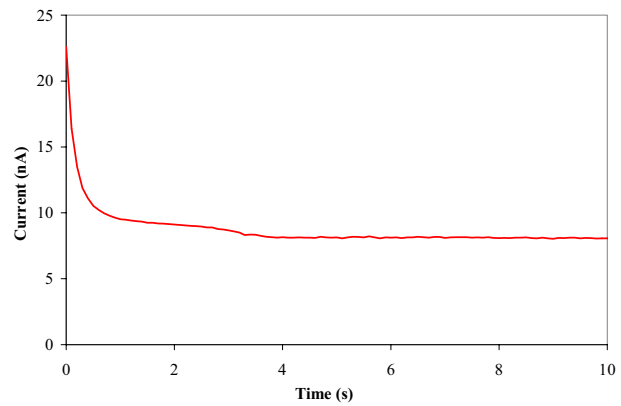
Fig. 8 Current collected versus time by a pinhole drilled in a Teflon insulated steel wire with 100 V applied to the wire.

There are actually several other elements that affect the current collection. Among these are the cleanliness of the collection area, the degree of contamination of the insulation, and the vapor content of the sample. When we do a measurement, the hole geometry itself is an issue. It is extremely difficult to make "perfect" holes at this small size for practical reasons. For example, the cuts through the insulation are not always smooth and rough edges remain, or the depth of the hole itself is not completely uniform. To be certain that the hole is completely through the insulation, we have to drill slightly to the metal. Consequently we will not have a smooth cylindrical surface anymore.

These are the reasons why it is difficult to come up with an exact scale factor able to relate the size of the drilled hole with the size of a ideal collecting sphere, so that electron saturation regime of the collecting hole matches the current collected by the equivalent sphere predicted by the oml model. It should be noted, however, that these issues are less pronounced at larger pinhole sizes.

Influence of Spacing

As a hypothesis, we reasoned that the spacing of the holes plays an important role in the current collection process. This idea is based on the concept of radius of influence. Here we show that, if our approach is correct, we should observe a decrease in the current collected by an array of holes once the radii of influence start to overlap. At that point, the current collection switches from a spherical collection mode to a cylindrical collection mode. The holes begin to interact with their neighbors and are no longer independent. When we have an array of holes close together such that they can "see" each other, one would expect them to interact. The presence of neighbors limits the plasma that can be collected by a hole if independent. Single holes see the plasma with a $\sim 2\pi$ solid angle while holes in an array have the plasma shadowed by their neighbors.

Sample Description

We used plain enamel-coated magnet wire, which is a solid bare copper conductor with a thin layer of oleoresinous insulation. The wire used has an outer diameter of 32 mil, which is smaller than the Debye length, but is large enough to drill an array of ten 15-mil-diameter holes in it. (Fig. 4) We used different spacing between holes and then recorded the corresponding I–V response.

Experimental Results

In this experiment, the Debye length is 1.9 mm, which is 75 mils. Figure 9 presents the current collected by 4 different samples each with 10 holes equally spaced at spacings of 25, 50, 75, and 100 mils. The current data was normalized to the 25-mil sample value at the plasma potential in order to eliminate variations due to hole size differences and the slight side-to-side variation of plasma density in the chamber. As expected, when the pinholes do not interfere with each other, the data tends to overlap. We see that the 25-mil spacing deviates earliest, followed by the 50-mil spacing data.

Comparison with Model

We wish to compare these experimental measurements to the one predicted by the theory presented earlier. So, we have to employ the plasma parameters for the present experiment. The electron density in this run is 1.5×10^{13} m^{-3}, the temperature is 1 eV. We consider a plasma potential on the order of 20 V. The equivalent radius given by Eq. (5) is not accurate here. Earlier, we considered an ideal situation and we introduced the scale factor $r_{\text{eff}} = r_h/\sqrt{2}$ assuming a perfect geometry. We discussed above that the insulation, the smoothness of the cut, and the degree of contamination also play important roles. Experimentally, the relation $r_{\text{eff}} = r_h/2.38$ gives a much better match. However, this value may change depending on a number of experimental factors, such as size of hole,
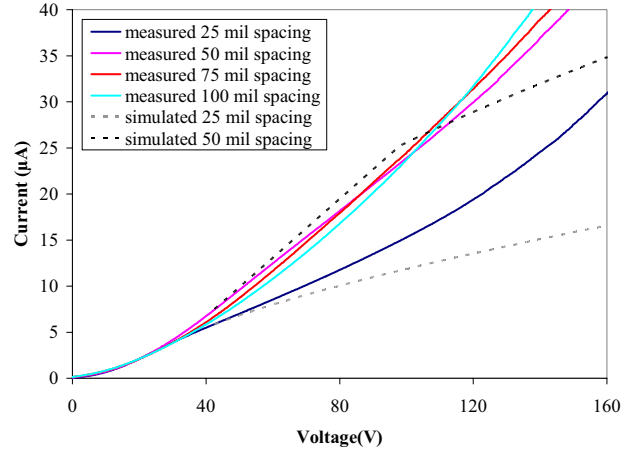
Fig. 9 **Normalized I–V characteristics of samples with equally spaced holes: 25, 50, 75, and 100 mils. Also included for comparison are the simulated currents collected by probes with 10 identical holes spaced by 25 and 50 mils.**

plasma density, shadowing effect, etc.

The current collected by the holes while they are independent is derived from Eq. (12) and is given by

$$I = 2\pi r_{\text{inf}}^2 j_{tk} N, \qquad (17)$$

where N is the number of holes. If a is the spacing between two consecutive holes, the potential value when the sheaths start to overlap is given by Eq. (7). These values are 30.3, 124.4, 281, and 500 V for 25, 50, 75 and 100 mils respectively. So, we expect the 25- and 50-mil spacings to show some shadowing effect in our experiment. Eq. (11) gives us the current collected by a length a as $I = j_{tk}\pi r_{\text{infl}}a$ when the sheaths are overlapping. We have $N-1$ such lengths. We also have one hole with no shadowing, which is really two halves given by the holes at each extremity of the array.

Above the threshold voltage with respect to the plasma potential, the current collected by this sample is given by

$$I = j_{tk}\pi r_{\text{infl}}a(N-1) + j_{tk}2\pi r_{\text{infl}}^2. \qquad (18)$$

Using Eq. (17) and Eq. (18) we can plot on the same figure the curves deduced from the model, with that of the measurement. For sake of visibility, we plot the theoretical curves for spacings of 25 and 50 mils and the measured curves corresponding, which are presented as well in Fig. 9. We can see that at $\sim$30 V, the 25-mil spacing current begins to drop indicating that the holes are no longer independent. We see a similar, although far less pronounced drop off in the 50-mil data at $\sim$100 V. The 75- and 100-mil spacing do not appear to be affected. The fact that the measured currents remain higher than the model current may be explained by the beginnings of secondary electron emission, which will be described below. We feel these

results show that our model is successful in predicting current levels by interfering holes.

It should be noted, however, that our model can be applied only in the electron or ion saturation regime. In the transition regime, called the electron retardation regime, the collection behavior is complex and we did not investigate theoretically the influence of the presence of a neighbor hole in the retardation regime.

We attempted to determine the influence of the spacing using other techniques and types of samples. We used stainless-steel wire insulated with Teflon tubing or polyolefin shrink wrap. We realized arrays of holes using several different techniques. We quickly discovered, however, that it was extremely difficult to realize clean holes with good repeatability. The problem lies with the size of the holes, which have to be much smaller than the Debye length, as well as with the nature of the insulation. Shavings remain after the hole has been drilled with most of the techniques used. The size and the orientation of these shavings have a great influence on the current collected due to plasma shadowing. We were unable to show this shadowing effect definitively with samples made in our initial attempts. We found that we needed a numerically controlled milling machine to be able to make holes clean enough to show this shadowing effect. This in itself leads to an interesting result, which is that the spacing between holes is a parameter much less important than the size of the holes.

One may also note that we expect the shadowing effect to appear at higher and higher voltages. However, at these high voltages, secondary electron emission may appear depending on the insulation used. Charged particles entering the sheath region are subject to motion constraints imposed on them by their own angular momentum. Part of them will miss the pinhole and strike the dielectric. If the energy of the colliding particle is above a certain energy threshold and below a certain energy maximum (determined by the bulk properties of the material) there is a high probability that more than one secondary electron will be liberated from the surface of the dielectric. Fig. 10 shows such an example. In this experiment we swept a stainless-steel wire insulated with oleoresinous insulation with 3 holes spaced greater than a Debye length apart. We used 3 holes in order to collect more current; the holes remained independent collectors. Up to ∼150 V, we have the I–V relation that we a expecting from spherical collectors. After 150 V, the current collected increases due to secondary electron emission. Around 220 V, there is a sharp increase, which is the snap over. At even higher voltages (not shown) above ∼350 V, arcing occurs.

### Current Collection to Severed Tether Lines

We are also interested in what the current–voltage characteristic is to a completely severed insulated wire.
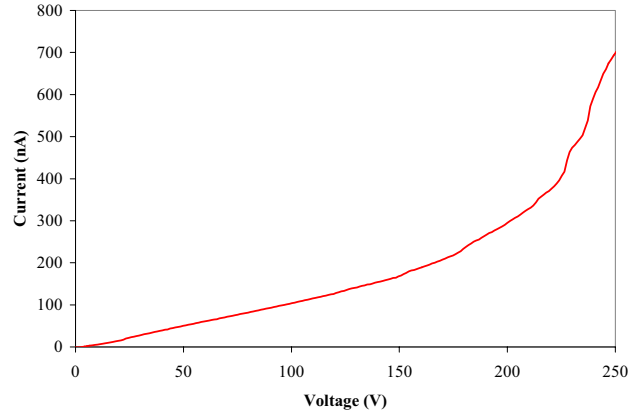
Fig. 10   I–V characteristics of a steel bar insulated with oleoresinous insulation with 3 spaced holes.

For these experiments we used a plain enamel-coated magnet wire and stainless-steel wire insulated with a Teflon and polyolefin tubing with the tip ends exposed to the surrounding plasma. Magnified views of the ends of these samples are shown in Fig. 11.
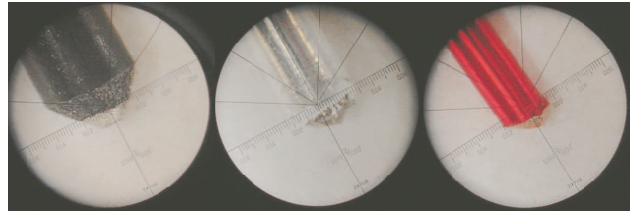

Fig. 11   Magnified views of samples simulating the severed end of an insulted tether; left to right: polyolefin-coated SS, Teflon-coated SS, enamel-coated copper.

Figure 12 shows the collected data for these samples. It is clearly seen that the I–V characteristics of exposed conductors at the end of insulated wire have a spherical current collection. The have the same shape as I–V from current collected to pinholes in insulation. The only difference is in the magnitude of the current collected, although this is related to the size of the holes compared to the collecting area of a cut wire. Still, although the geometry is different, the collection process is similar to current collection by pinhole. Therefore, it would appear to be difficult with this information alone to differentiate a cut tether from a tether having breaches.

Conclusions

In this study we characterized the current collection of pinholes in insulated conductors. These simulated tethers have radii less than the Debye length of the plasma they are immersed in, so the dimensions of the holes are also smaller than the Debye length. I–V sweeps indicate that they do have spherical-like current collection as predicted. We investigated the influence of the size of the hole. A good first-order approximation is given by a linear relation between
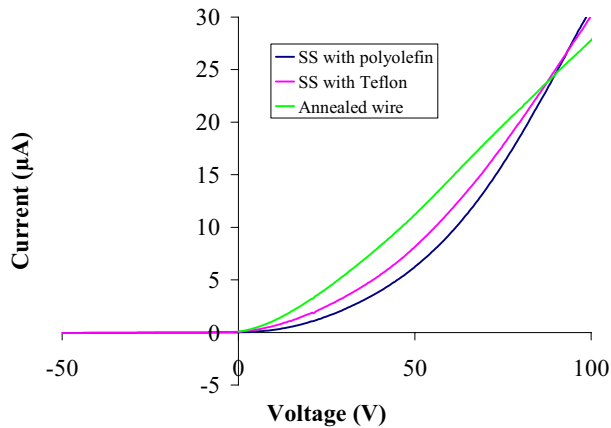
Fig. 12   I–V characteristics of a exposed wire at the end of insulated conductors.

the area exposed and the current collection. However, there are other factors that play a role. We noted that the presence of the insulation has a nonlinear effect by geometrically shadowing the plasma. The presence of the insulation also acts as a capacitor, but it is difficult to quantify this effect exactly.

We developed a model for the current collection to an array of pinholes. This model accounts for the interaction of the neighboring holes on the current collection. We introduced the concept of radius of influence. The model switches from a spherical to a cylindrical-like current collection as the applied voltage is increased beyond a threshold value. We then compared our model to experiment. We tested several samples with arrays of different hole spacings. We were able to see that the experiments show the trend given by the model and with an appropriate scale factor, the match is fairly good.

In this study, we limited ourselves to the I–V characteristic of the holes. To measure the state of heath of a tether, the next step will be to develop a circuit model for the faults. This will allow the use of a simulation program like HSPICE. Important studies have been done to model the tether as a transmission line. Pulse propagation along conductor in low density plasma has been studied.[17] With a model for the transmission line and the breaches it will be possible to focus on the inverse problem of locating and measuring the breaches. The use of time-domain reflectometry (TDR) has been proposed to determine fault position and/or density along electrodynamic tether (EDT) systems.[18,19] The TDR technique has long been an effective tool for determining the location of loads and faults along common transmission lines such as coaxial cables. Including a TDR system as part of long-duration EDT missions would facilitate real-time tracking of the expected performance degradation and health state of the tether. In addition, the models developed here will allow us to predict performance loss for propulsive tether systems due to current leakage.

This study also opens the way to new applications. We can consider the possibility of using a tether with calibrated holes along its length to have an *in situ* measurement of the ionospheric plasma. It would be a novel diagnostic complementing bulk measurement done with more traditional devices.

Acknowledgments

References

[1]Hoyt, R. P., "Design and Simulation of a Tether Boost Facility for LEO to GTO Transport," *AIAA Paper 2000–3866*, 2000.

[2]Santangelo, A., and Johnson, L., "Future Applications of Electrodynamic Tethers for Propulsion," *AIAA Paper 2000–3870*, 2000.

[3]Vas, I. E., Kelly, T. J., and Scarl, E. A., "Space Station Reboost with Electrodynamic Tethers," *J. Spacecr. Rockets*, Vol. 37, 2000, pp. 154–164.

[4]Anz–Meador, P. D., "Tether-Debris Interactions in Low Earth Orbit," in proceedings of *Space Technology and Applications International Forum (STAIF-2001)*, edited by M. El-Genk, AIP Conference Proceedings 552, American Institute of Physics, New York, 2001, pp. 525–531.

[5]Forward, R. L., "Failsafe Multistrand Tether Structures for Space Propulsion," AIAA Paper 92–3214, 1992.

[6]Johnson, Les, Gilchrist, Brian E., Estes, Robert D., Lorenzini, Enrico, and Ballance, Judy, "Propulsive Small Expendable Deployer System (ProSEDS) Space Experiment," AIAA Paper AIAA–98–4035, 1998.

[7]Gilchrist, B. E., Ballance, J., Curtis, L., Johnson, L., and Vaughn, J., "The Propulsive Small Expendable Deployer System (ProSEDS) Experiment: Preparing for Flight," *International Electric Propulsion Conference*, Pasadena, CA, 14–19 October 2001.

[8]Vayner, B., Galofaro, J., Ferguson, D., and de Groot, W., "The Conductor–Dielectric Junctions in a Low Density Plasma," *38th AIAA Aerospace Sciences Meeting and Exhibit,* Reno, NV, Jan. 2000.

[9]Kennerud, K. L., "High Voltage Solar Array Experiments," NASA CR–121280, March 1974.

[10]Herr, J., and Snyder, D., "Plasma Sheath Effects on Ion Collection by a Pinhole," AIAA 93–0567, *31st AIAA Aerospace Sciences Meeting and Exhibit,* Reno, NV, Jan. 1993.

[11]Galofaro, J. T., "Comparison of Current Predicted by NASCAP/LEO Model Simulations with Elementary Langmuir-Type Bare Probe Models for an Insulated Cable Containing a Single Pinhole," *NASA Technical Memorandum 102486*, July 1990.

[12]Mathews, J. D., Meisel, D., Hunter, K.P., Getman, V.S., and Zhou, Q., "Very High Resolution Studies of Micrometeors Using the Arecibo 430 MHz Radar," *Icarus,* Vol. 126, 1997, pp. 157–169.

[13]Lai, S.T., Murad, E., and McNeil, W., "Hazards of Hypervelocity Impacts on Spacecraft," *J. Spacecraft and Rockets,* Vol. 39, Iss. 1, 2002, pp. 106–113.

[14]Sanmartín, J. R., Martinez-Sánchez, M., and Ahedo, E., "Bare Wire Anodes for Electrodynamic Tethers," *J. of Prop. and Power*, Vol. 9, No. 3, 1993, pp. 353–360.

[15]Sanmartín, J. R., and Estes, R. D., "The Orbital-Motion-Limited Regime of Cylindrical Langmuir Probes," *Physics of Plasmas*, Vol. 6, No. 1, 1999, pp. 395–405.

[16]Estes, R. D., and Sanmartín, J. R., "Cylindrical Langmuir Probes Beyond the Orbital-Motion-Limited Regime," *Physics of Plasmas*, Vol. 7, No. 10, 2000, pp. 4320–4325.

[17]Bilén, S. G., *Pulse Propagation along Conductors in Low-Density, Cold Plasmas as Applied to Electrodynamic Tethers in the Ionosphere*, Ph. D. Thesis, The University of Michigan, 1998.

[18]Bilén, S. G., and B. Gilchrist, "Electrodynamic-Tether Time-Domain Reflectometer for Analyzing Tether Faults and Degradation," in proceedings of *Space Technology and Applications International Forum (STAIF-2001)*, edited by M. El-Genk, AIP Conference Proceedings 552, American Institute of Physics, New York, 2001.

[19]Bilén, S. G., and Kern, O., "Electrodynamic-Tether Fault Measurement using Time-Domain Reflectometry," in proceedings of *Space Technology and Applications International Forum (STAIF-2001)*, edited by M. El-Genk, AIP Conference Proceedings 552, American Institute of Physics, New York, 2002.